Supporting Information

Co, N-codoped nanotube/graphene 1D/2D heterostructure for efficient oxygen reduction and hydrogen evolution reactions

Liu Yang[1,2], Yanlong Lv[2], Dapeng Cao[1,2,*]

[1] Beijing Advanced Innovation Center for Soft Matter Science and Engineering, Beijing University of Chemical Technology, Beijing 100029, People's Republic of China

[2] State Key Laboratory of Organic-Inorganic Composites, Beijing University of Chemical Technology, Beijing 100029, People's Republic of China

***Corresponding author. Email: caodp@mail.buct.edu.cn**

1. Experiments

1.1 Materials

Urea (95%, Alfar Aesar), $CoCl_2$ $6H_2O$ (Alfar Aesar) and HCl were purchased from Beijing Chemical Works. High-purity nitrogen gas was provided from Beijing AP BAIF Gases Industry Co. Ltd.

1.2 Synthesis of Co/NG, Co/NCNT/NG and Co/NCNT

0.2 g g-C_3N_4 was dissolved in 50 ml deionized water, sonicated to make it completely dissolved. Then 1.2 ml (0.17 M $CoCl_2$ $6H_2O$) was injected into above solution. The well disperse solution continued to stir 24h then the solution was evaporated at 80℃. The dried sample was carbonized at 550℃ for 2h with the heating

rate 2 ℃/min and then continue heated to 800℃ for 2h with the heating rate 2 ℃/min in a N_2 atmosphere. The final product was labelled as Co/NCNT/NG catalyst. As a comparison, the Co/NG and Co/NCNT catalyst were obtained from above procedures with adding 0.6 ml, 2.4 ml (0.17 M $CoCl_2$ $6H_2O$), respectively.

2. Characterization

Scanning electron microscope (SEM) images were obtained on HITACHI S-4800 instrument. High-resolution transmission electron microscope (HRTEM) images were recorded on a TECNAI G2 F20 field emission transmission electron microscope at 200 kV, which equipped with an energy dispersive spectrometer (EDS) analyzer. Powder X-ray diffraction (PXRD) measurements were performed by a D8 ADVANCE X-ray diffractometer with Cu Kα line (λ =1.54178 Å). Raman spectra were received through a LabRAM Aramis Raman Spectrometer. N_2 adsorption/desorption analysis was measured by an ASAP 2460 analyzer (Micromeritics, U.S.A) at 77 K. Pore size distribution was calculated by density functional theory (DFT). X-ray photoelectron spectroscopy (XPS) measurements were carried out by a Thermo Fisher ESCALAB 250 X-ray photoelectron spectrometer equipped with using 150 W Al Kα radiation.

X-ray Absorption Fine Structure (XAFS) was measured in Beijing Synchrotron Radiation Facility on the beamline 4W1B, (BSRF) China. The storage rings of BSRF were operated at 2.5 GeV with a maximum current of 250 mA. EXAFS data were collected using a fixed-exit double-crystal Si (111) monochromator. Co Kedge EXAFS data were analyzed using standard procedures with the program IFEFFIT.

3. Electrochemical measurements

To evaluate ORR performance, all the electrochemical measurements were performed in a standard three-electrode system on a CHI760e electrochemical workstation using a glassy carbon (GC, area of 0.196 cm^2), in which saturated calomel electrode (SCE) regarded as a reference electrode, 1 cm^2 platinum net as a counter electrode and and 0.1M KOH solution as electrolyte. For testing HER performance, all operation is the same as above except using carbon rods as a counter electrode and employing 0.5 M H_2SO_4 as electrolyte. All of the potentials were calibrated to the reversible hydrogen electrode (RHE) in the light of Nernst equation. The potential range is cyclically scanned between -1.0 to 0 V for ORR in alkaline solution and -0.9 to -0.25 V for HER in acidic solution. RDE and RRDE measurements were conducted by using an American Pine Instruments device.

For fabrication of the working electrode, 5 mg synthesized carbon catalysts or commercial 20% Pt/C dispersed in 0.2 mL ethanol and 0.8 mL deionized water, then added into 50 μL of 5 wt% Nafion solution. The mixed solution was sonicated for at least 30 min to form a homogeneous dispersion then dried under room temperature. All prepared catalysts were deposited on the GC with loading of 10μL (~ 0.24 mg cm-2) in various electrolytes. The iR compensated (80%) was applied to remove the influence of the Ohmic resistance for HER. Cyclic voltammetry (CV) and linear sweep voltammetry (LSV) were conducted in 0.1 M KOH or 0.5 M H_2SO_4 aqueous solutions. The RRDE examinations were carried out with the Pt ring electrode to test the ring current (I_{ring}). The peroxide yield (HO_2^- %) and the electron transfer number

(n) were calculated by

$$n = 4 \times \frac{I_{disk}}{\left(\frac{I_{ring}}{N}\right) + I_{disk}}$$

$$H_2O_2(\%) = 200 \times \frac{I_{ring}}{\left(\frac{I_{ring}}{N}\right) + I_{disk}}$$

I_{disk} is the disk current, and I_{ring} is the ring current. N is the current collection efficiency of the Pt ring that is 0.42.

The kinetics parameters were calculated using Koutecky–Levich equations ：

$$\frac{1}{J} = \frac{1}{J_L} + \frac{1}{J_K} = \frac{1}{J_K} + \frac{1}{B\omega^{1/2}}$$

$$B = 0.62nFC_0D^{2/3}\upsilon^{-1/6}$$

where J is the measured current density, J_k, J_L are the kinetic- limiting current densities and diffusion-limiting current densities, respectively. ω is the angular velocity. F is the Faraday constant (F 96500 C/mol). C_0 is the bulk concentration of O_2 in 0.1 M KOH (mol/cm^3). D is the diffusion coefficient of O_2 in 0.1 M KOH and 0.5M H_2SO_4 solution cm^2/s). υ is the kinematic viscosity of the electrolyte (0.01 cm^2/s) and k is the electron-transfer rate constant.

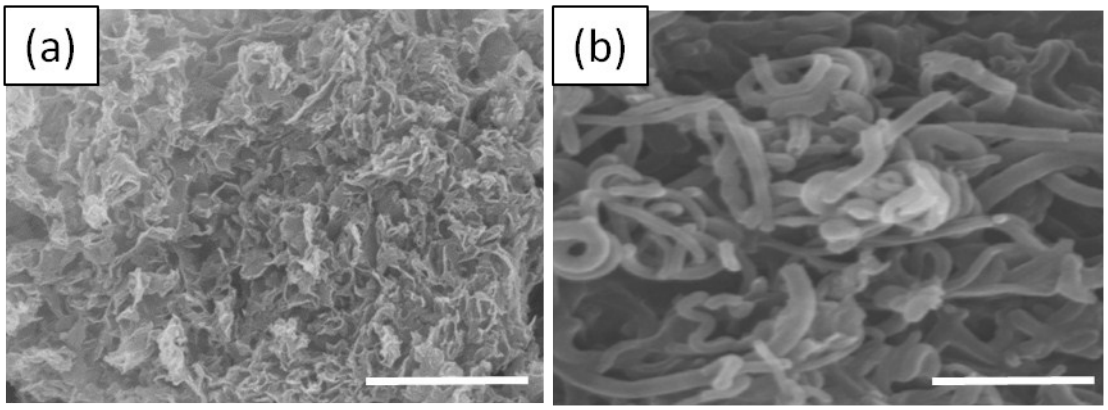

Figure S1 (a) SEM image of Co/NG. (scale bar, 1 μ m) **(b)** SEM image of Co/NCNT. (scale bar, 400 nm)

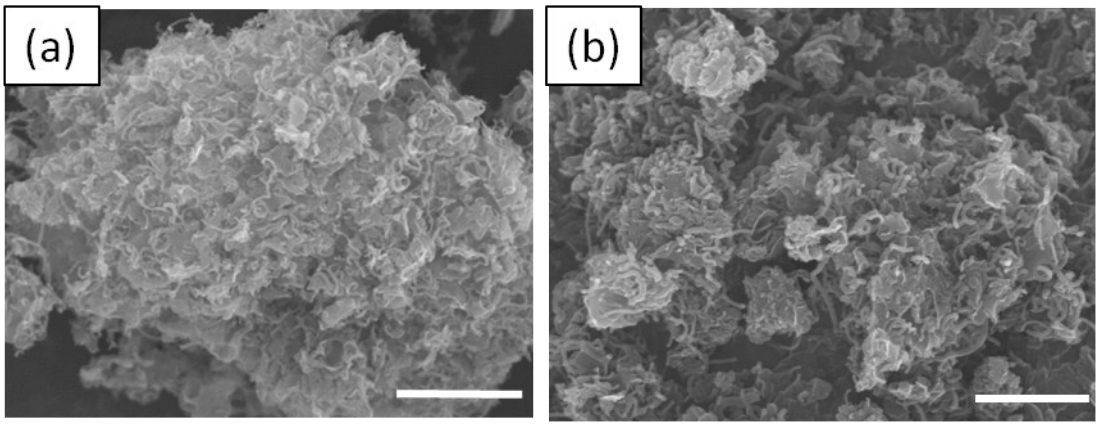

Figure S2 (a) (b) SEM images of Co/NCNT/NG. (scale bar, 1 μ m)

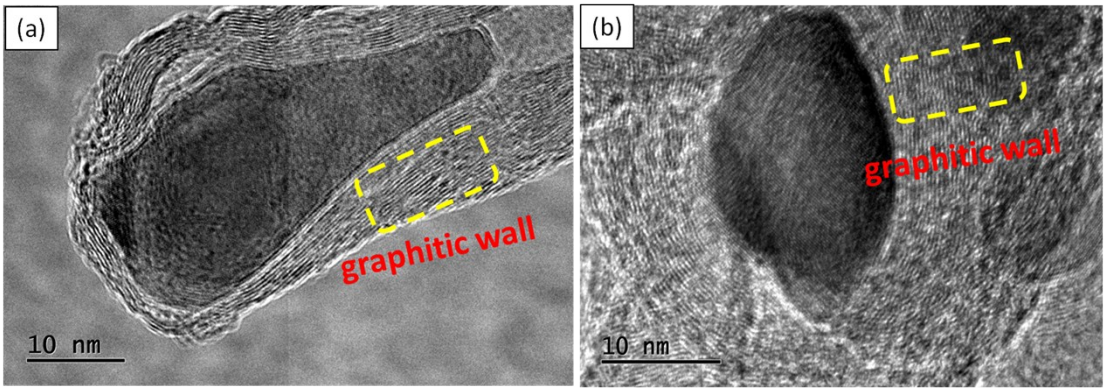

Figure S3 (a) (b) TEM images of Co/NCNT/NG.

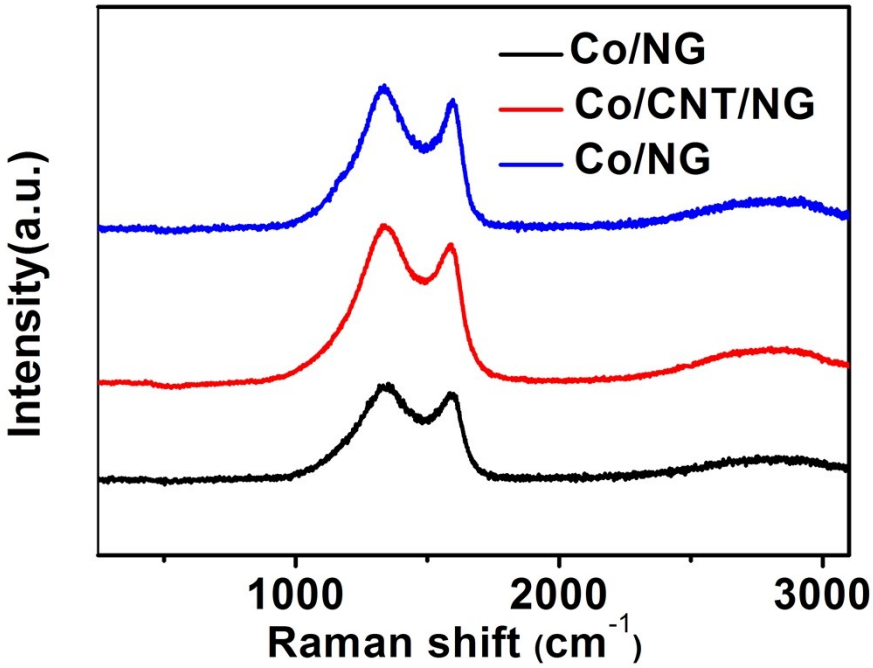

Figure S4 The Raman spectrum of Co/NG, Co/NCNT/NG and Co/NCNT.

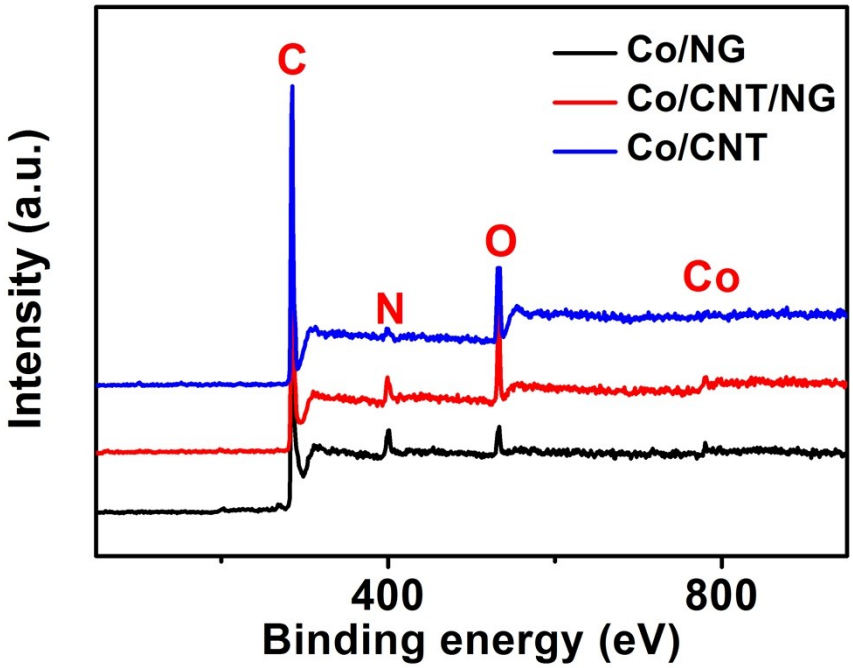

Figure S5 XPS spectra of Co/NG, Co/NCNT/NG and Co/NCNT.

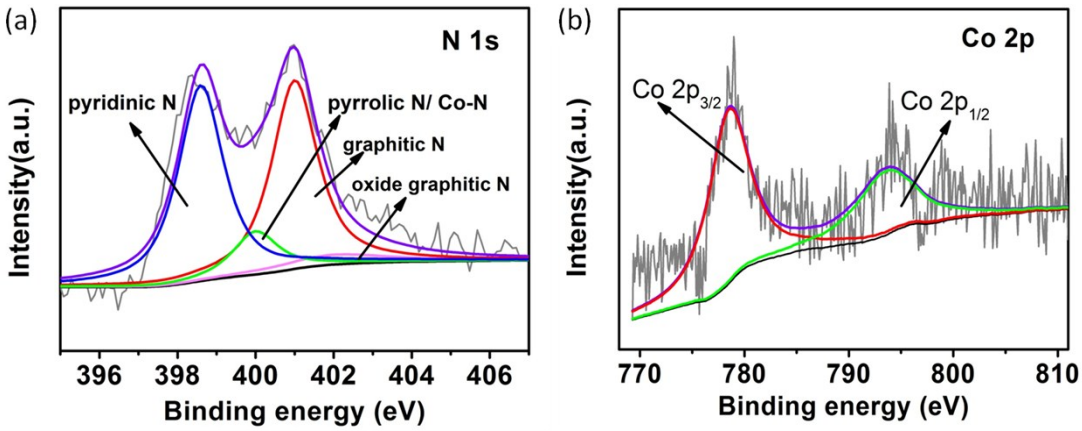

Figure S6 (a) High-resolution XPS spectra of N 1s **(b)** Co 2p for Co/NG.

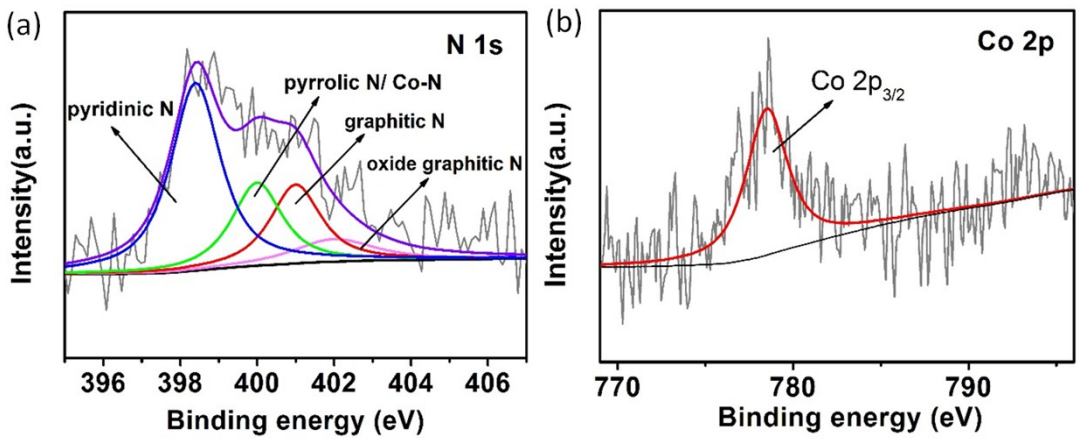

Figure S7 (a) High-resolution XPS spectra of N 1s **(b)** Co 2p for Co/NCNT.

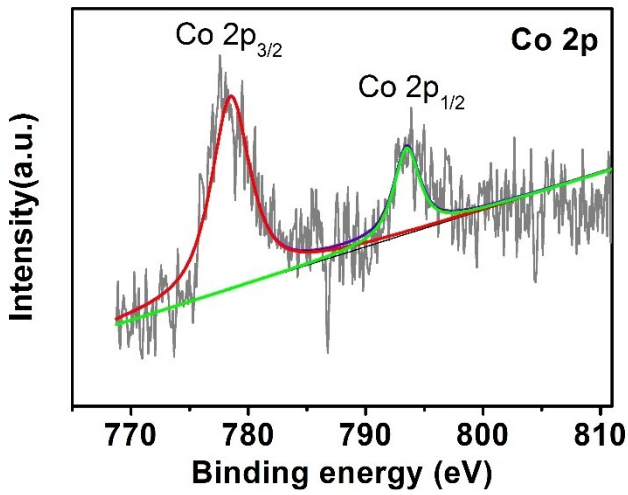

Figure S8 High-resolution XPS spectra of Co 2p for Co/NCNT/NG.

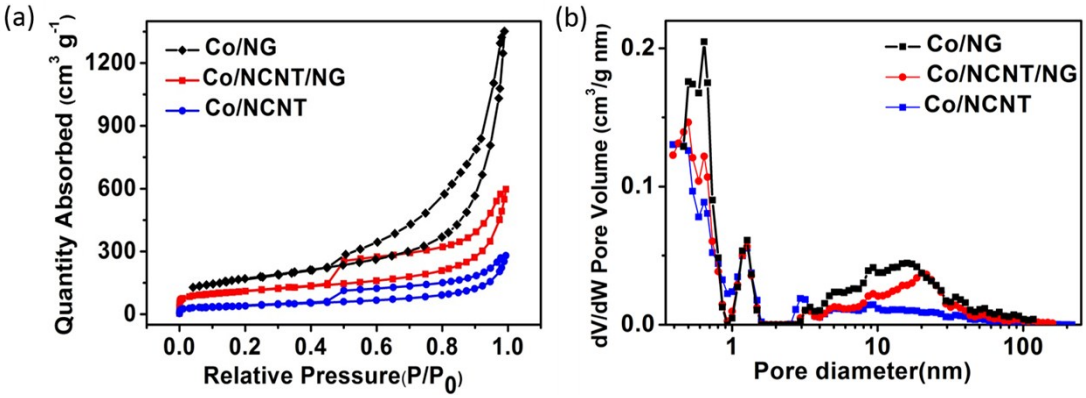

Figure S9 (a) N_2 adsorption–desorption isotherms at T=77 K and **(b)** the pore size distributions of Co/NG, Co/NCNT/NG and Co/NCNT.

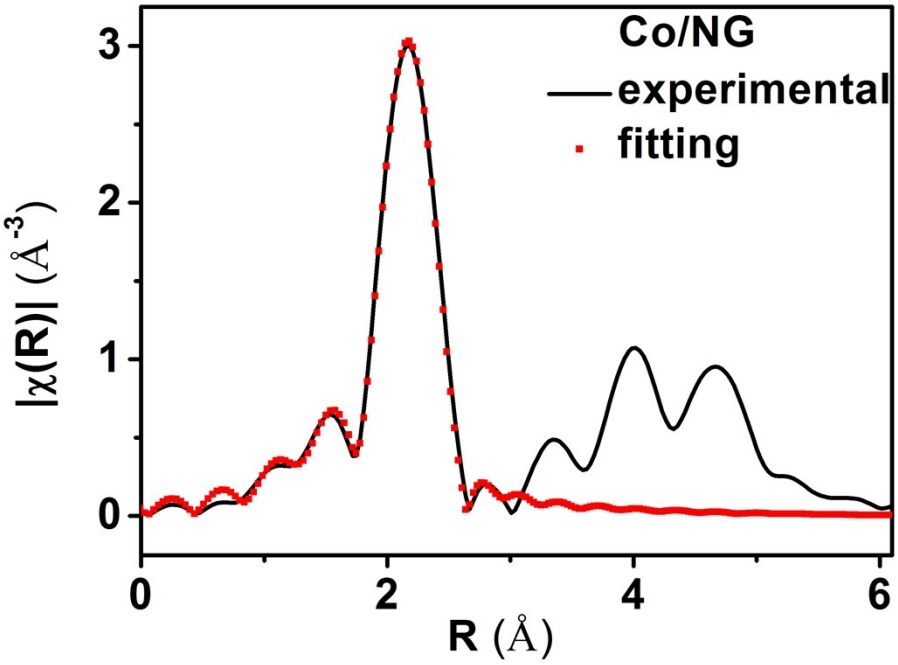

Figure S10 Fourier-transformed of Co K-edge spectra of Co/NG and corresponding fitting.

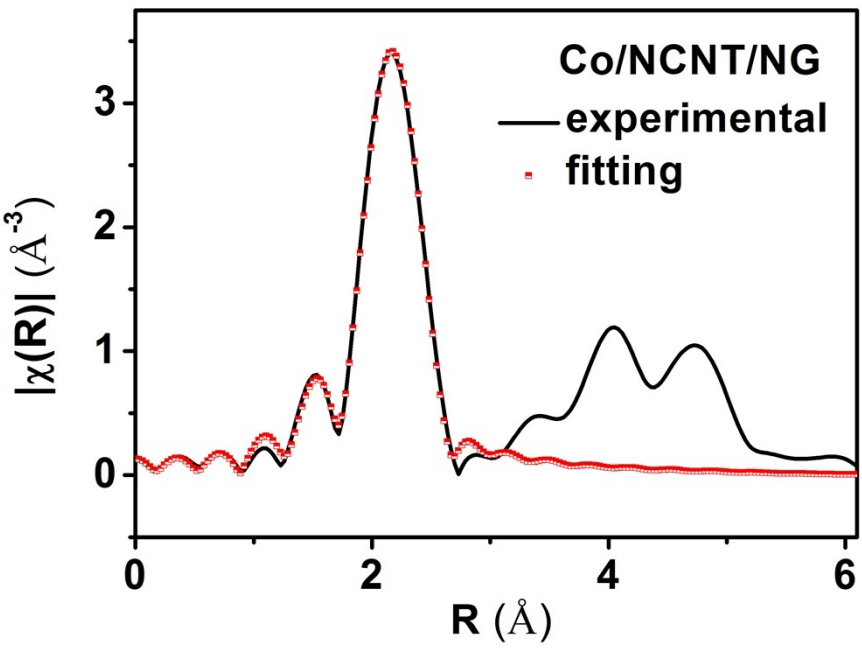

Figure S11 Fourier-transformed of Co K-edge spectra of Co/NCNT/NG and corresponding fitting.

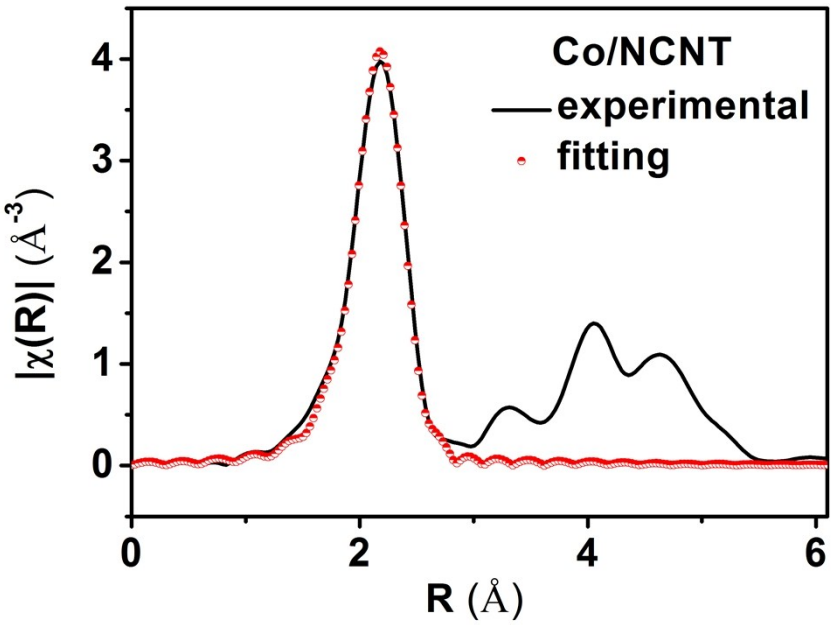

Figure S12 Fourier-transformed of Co K-edge spectra of Co/NCNT and corresponding fitting.

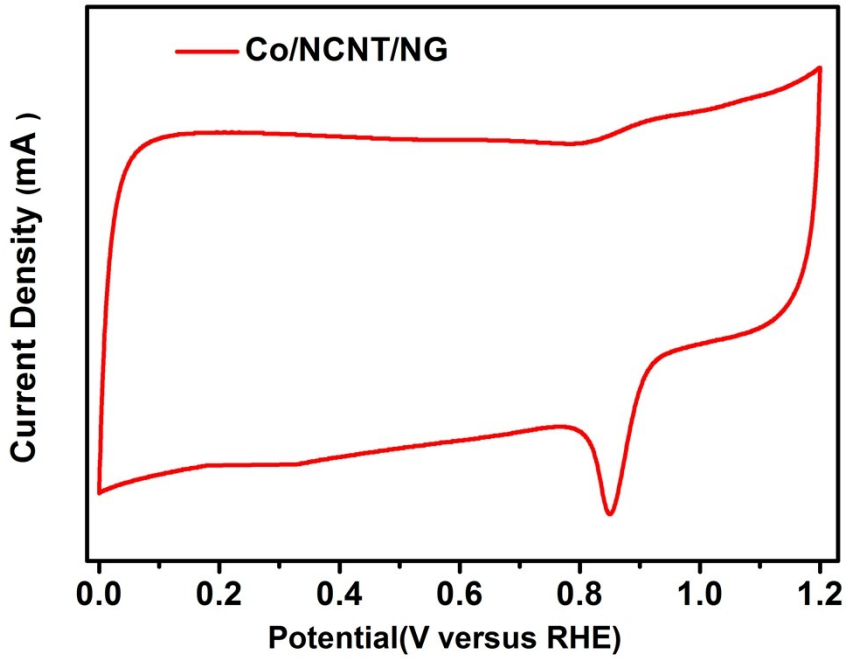

Figure S13 CV curve of Co/NCNT/NG in in O_2-saturated 0.1 M KOH.

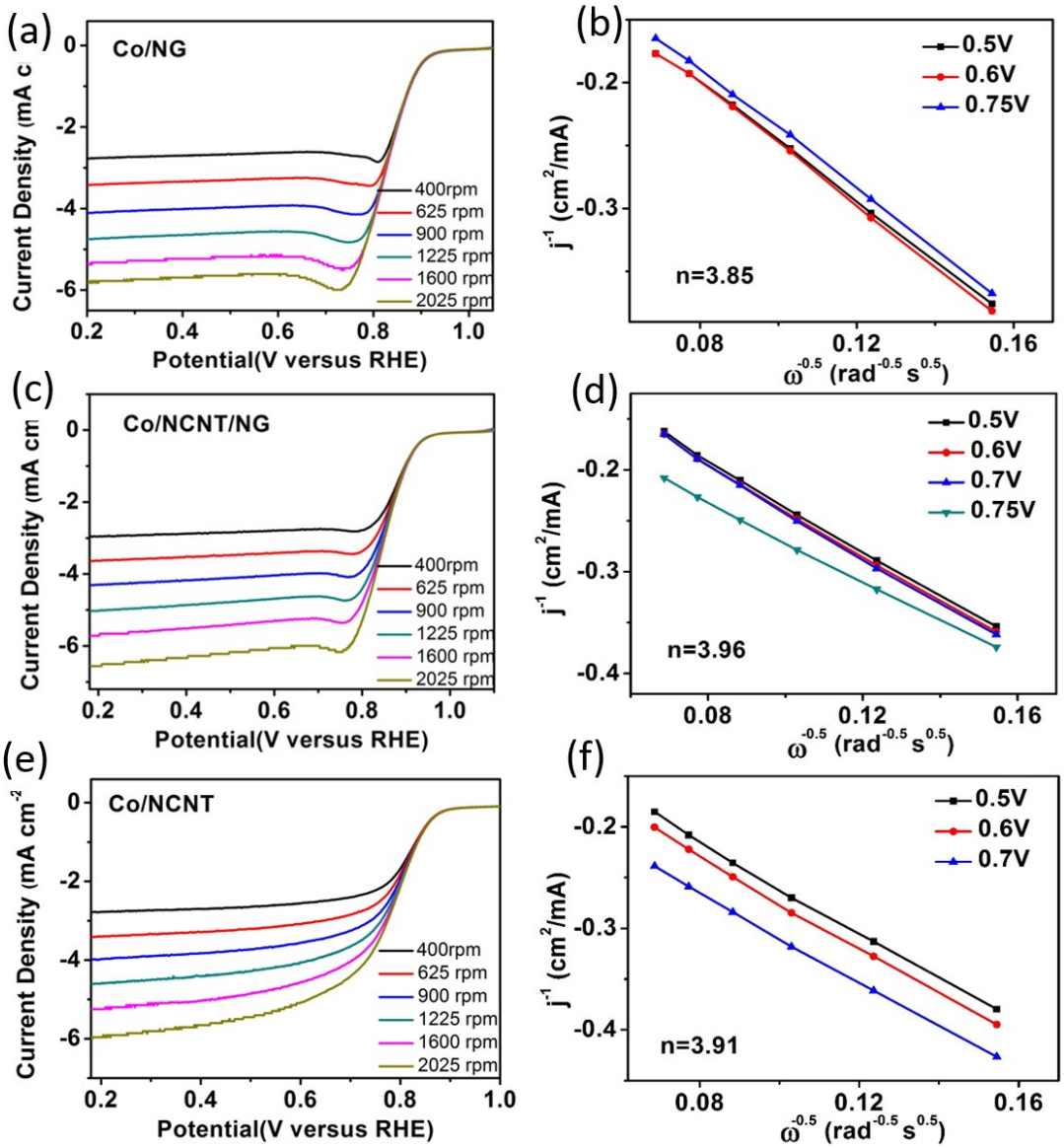

Figure S14 RDE LSV of Co/NG **(a)**, Co/NCNT/NG **(c)** and Co/NCNT **(e)** at different rotating speeds in O_2-saturated 0.1 M KOH solution at the various rotating rates (400 rpm-2025 rpm). Corresponding Koutecky-Levich plots of Co/NG **(b)**, Co/NCNT/NG **(d)**, Co/NCNT **(f)** derived from RDE at different potentials.

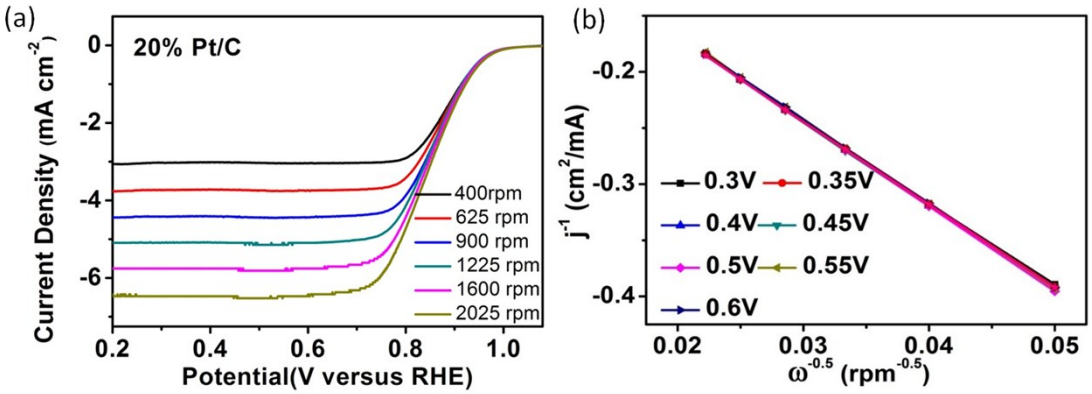

Figure S15 (a) RDE LSV of 20% Pt/C and **(b)** corresponding Koutecky-Levich plots.

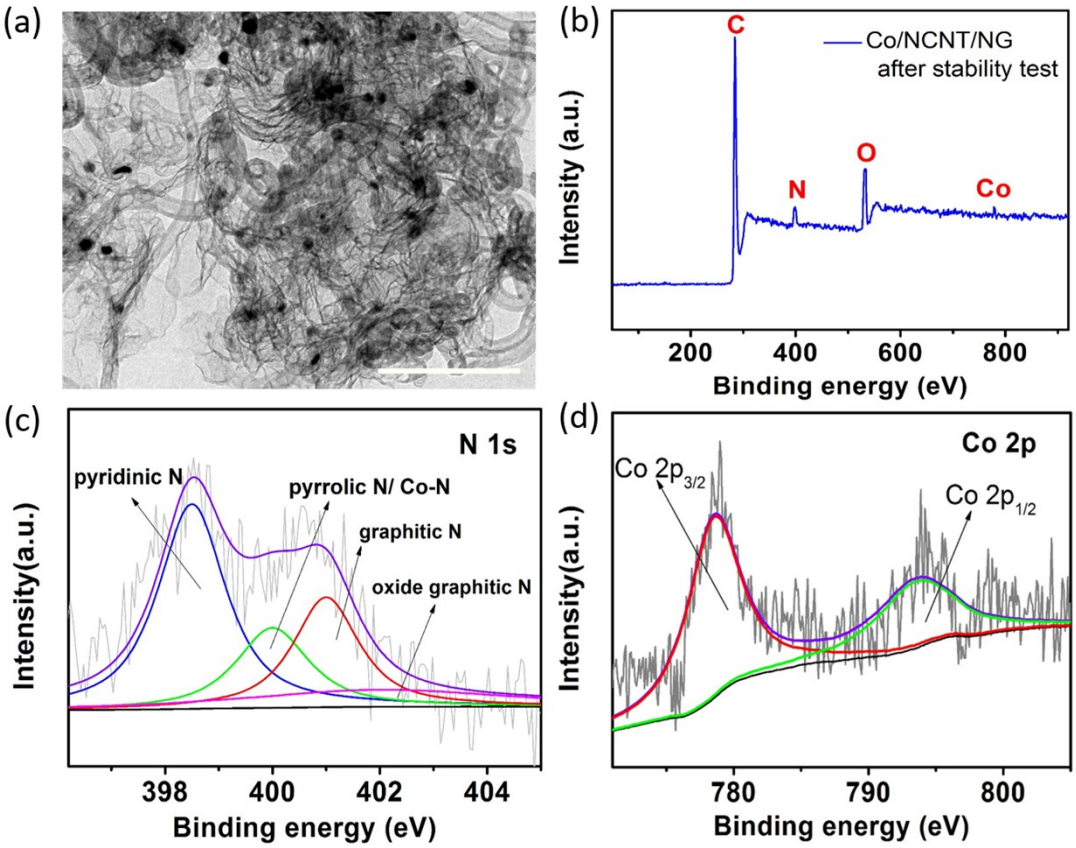

Figure S16 (a) TEM image of Co/NCNT/NG after 20 hours ORR durability test, scale bar 200 nm. **(b)** XPS spectra **(c)** High-resolution XPS spectra of N 1s and **(d)** Co 2p of Co/NCNT/NG after 20 hours ORR durability test.

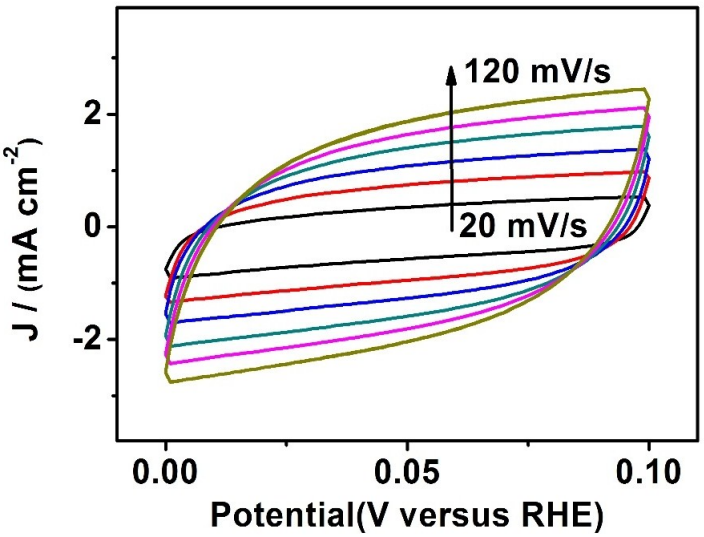

Figure S17 CV curves of Co/NCNT/NG at 0-0.1 V, the scanning rate ranging from 20-120 mV/s.

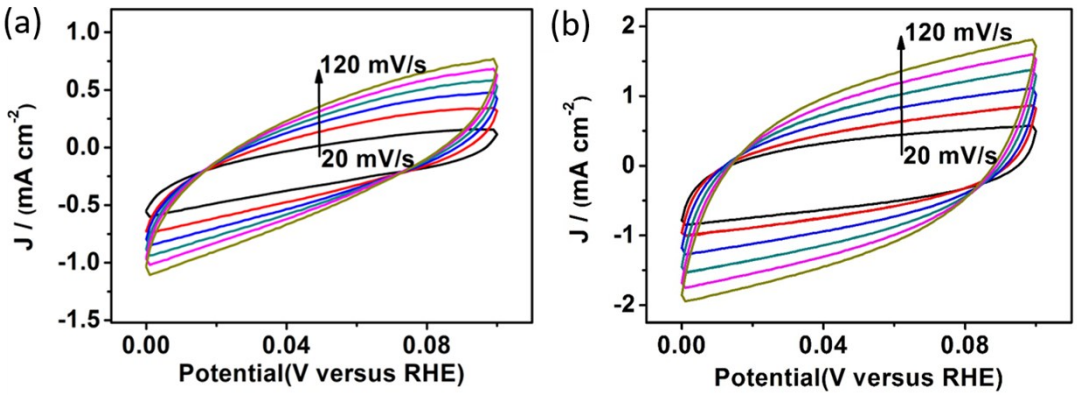

Figure S18 (a) CV curves of Co/NG and **(b)** Co/NCNT at 0-0.1 V, the scanning rate ranging from 20-120 mV/s.

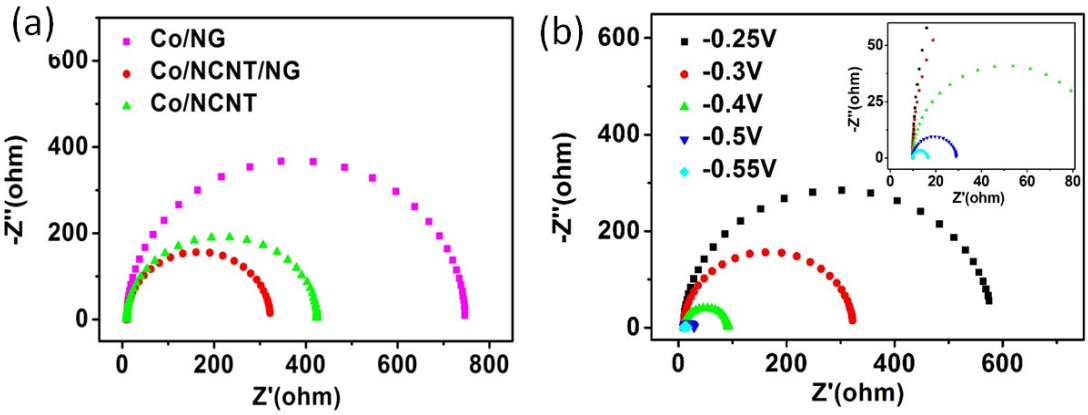

Figure S19 (a) Electrochemical impedance spectroscopy (EIS) of Co/NG, Co/NCNT/NG and Co/NCNT at η=300 mV. (b) EIS of Co/NCNT/NG at different overpotentials.

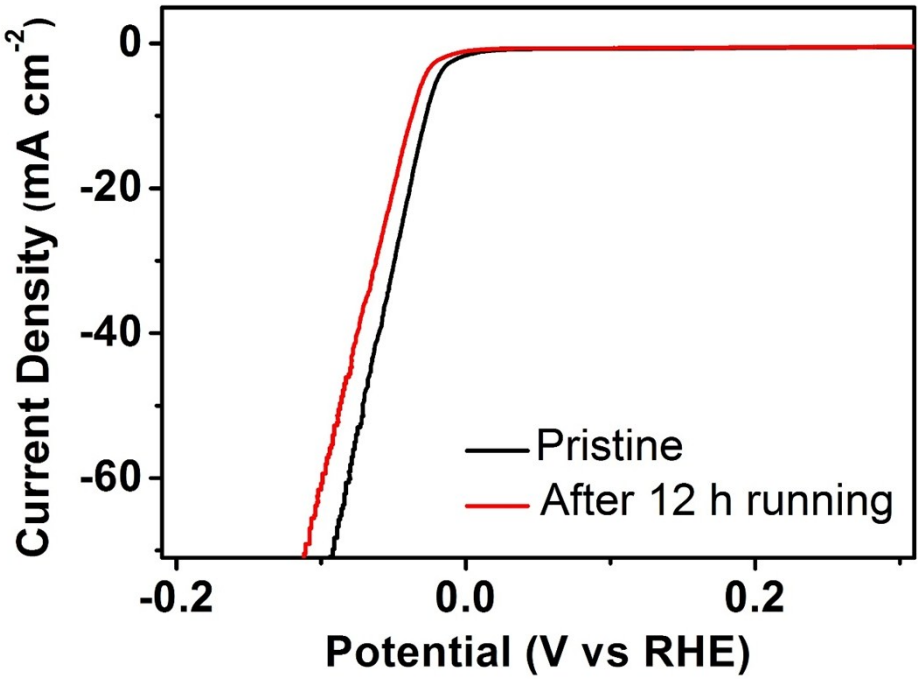

Figure S20 HER polarization curves of 20% Pt/C before and after 12 h CV cycles at an RDE rotation rate of 1600 rpm in O_2 saturated 0.5 M H_2SO_4 solution.

Table S1 Summary of XPS elemental analysis of three samples.

Percentage(%)	C[%]	N[%]	O[%]	Co[%]	pyridinic N [%]	pyrrolic N/ Co-N [%]	graphitic N [%]	Oxide graphitic N [%]
Co/NG	90.8	2.6	6.2	0.4	43.4	9.6	41.8	5.2
Co/NCNT/NG	86.6	**5.9**	6.7	**0.8**	**49.8**	17.5	19.8	12.9
Co/NCNT	90.4	2.47	5.52	0.7	48.6	21.5	20.4	9.5

Table S2 Summary of porosity parameters of three samples.

Samples	S_{BET} ($m^2 g^{-1}$)	Vt ($cm^3 g^{-1}$)	Pore size (nm)
Co/NG	588.1	1.96	11.7
Co/NCNT/NG	371.8	0.92	9.5
Co/NCNT	143.7	0.43	12

Table S3 Parameters of EXAFS fits for three samples.

sample	path	Coordination Number	Bond length R (Å)	Bond disorder σ^2 (10^{-3} Å^2)	R factor (%)
Co/NG	Co-N	1.5	1.93	4.6	0.62
	Co-Co	3.6	2.49	3.1	
Co/NCNT/NG	Co-N	2.0	1.93	3.4	0.54
	Co-Co	4.2	2.6	3.1	
Co/NCNT	Co-N	0.8	1.93	6.1	0.20
	Co-Co	6.1	2.49	2.6	
Co foil	Co-Co	12.0	2.49	4.7	0.36

Table S4 HER performance of Co/NCNT/NG and other Co-based electrocatalysts in acidic media (* catalysts directly grown on current collectors).

Catalysts	On-set potential (mV)	Overpotential at 10 mA/cm^2	Refs.
Co@CNT	50	260	Angew. Chem. Int. Ed. 2014, 53, 4372 –4376
FeCo@N-doped Carbon	70	270	Energy Environ. Sci., 2014, 7, 1919–1923
$Co_{0.6}Mo_{1.4}N_2$	-	200	J. Am. Chem. Soc. 2013, 135, 19186 −19192
CoNi@NC	~ 0	142	Angew. Chem. Int. Ed. 2015, 54, 2100 –2104
Co@NCNT/CC*	-	78	ChemSusChem 2015, 8, 1850
CoP mesoporous carbon	77.74	112	J. Mater. Chem. A 2015 , 3 :4255-4265
CoS_2/RGO-CNT	100	142	Angew. Chem. Int. Ed. 2014, 53, 12594 –12599
CoNx/rGO	30	142	Nat. Commun. 2015, 6, 8668
CuCo@NC	115	145	Adv. Energy Mater. 2017, 1700193
$CoSe_2$ NP/CP*	-	139	J. Am. Chem. Soc. 2014, 136, 4897
Co-NRCNTs	50	260	Angew. Chem. Int. Ed. 2014, 53, 4372
CoP/CC*	38	67	J. Am. Chem. Soc. 2014, 136, 7587−7590
Cobalt NPs on N−Dope Graphene Nanosheets	-49	200, J=13.6 mA/cm2	Chem. Mater. 2015, 27, 2026−2032
Co/CoP/carbon membranes	-	138	ACS Nano 2017, 11, 4358−4364
Co−C−N	-	138	J. Am. Chem. Soc. 2015, 137,15070− 15073
Co_9S_8@MoS_2	64	190	Adv. Mater. 2015, 27, 4752-4759
Co/NCNT/NG	59	123	This work